

Sorption–desorption properties of nitric oxide over

 $\text{La}_{2-x}\text{Sr}_{1+x}\text{Cu}_2\text{O}_{6-\delta}$ ($0 \leq x \leq 2$)

Masato Machida,* Nobuyuki Masuda and Tsuyoshi Kijima

Department of Material Sciences, Faculty of Engineering, Miyazaki University, 1-1 Gakuen-Kibanadai, Miyazaki 889-2192, Japan. E-mail: machida@material.chem.miyazaki-u.ac.jp

Received 22nd December 1998, Accepted 9th March 1999

The NO sorption/desorption properties of substituted layered cuprates, $\text{La}_{2-x}\text{Sr}_{1+x}\text{Cu}_2\text{O}_6$, have been studied to use them as an NO_x storage material. The cumulative amount as well as the initial rate of NO uptake at 250 °C increased with Sr-substitution, x , giving rise to the maximum at $x=1.4$, where a mixture of a orthorhombic layered cuprate and two binary oxides (Sr_2CuO_3 and SrCuO_2) was produced. The latter binary oxides play a key role in promoting the oxidation of NO and thus solid–gas reactions with the layered cuprate phase, which is accompanied by the formation of nitrate and nitrite species. The absorbed NO was liberated reversibly when heated at 200–600 °C in a stream of He. Sorption/desorption of NO could be cycled by employing a temperature-swing operation. The NO reactivity of the $\text{La}_{2-x}\text{Sr}_{1+x}\text{Cu}_2\text{O}_6$ system is compared with that of the $\text{La}_{2-x}\text{Ba}_x\text{SrCu}_2\text{O}_6$ system in our previous study, which shows NO uptake based on intercalation into the layered structure and dissociative desorption to produce N_2 and O_2 .

Introduction

A sorption/desorption cycle is useful for removing dilute NO_x in gas exhausts.^{1,2} Recent progress in catalytic NO_x conversion has stimulated the novel application of NO_x storage materials, which is exemplified by a NO_x storage three-way catalyst for automotive lean-burn engines developed by Toyota Motor Corporation.³ Much attention has been directed toward utilizing solid sorbents for trapping NO_x in the presence of oxygen.⁴ Prior to these studies, several research groups have already pointed out that various transition metal oxides containing alkaline-earth elements possess potential abilities for sorptive NO_x removal.^{5–10} These studies suggested that various solid- NO_x interactions, such as adsorption, complex formation, nitrate (nitrite) formation, and/or direct incorporation, are a promising basis for the sorptive removal.

In our previous publications,^{11–15} we have reported a novel NO-solid reaction based on intercalation into Ba-substituted double layered cuprates, $\text{La}_{2-x}\text{Ba}_x\text{SrCu}_2\text{O}_6$. This material can accommodate NO molecules into the interlayer up to *ca.* 1 mol (mol-Ba)⁻¹ at 250 °C. More interestingly, the deintercalation process at higher temperatures results in significant N_2 emission at > 800 °C as a result of dissociative desorption of intercalated NO. This irreversible NO sorption/desorption is associated with NO-oxygen defect interactions in the intercalation compound and is not observed in any other metal oxide systems so far reported. We have also demonstrated that such sorption/desorption cycles can be repeated by means of a temperature swing operation.¹⁵ The NO uptake in this system is driven by an equimolecular interaction with Ba as for other Ba-based NO_x storage materials.^{1,8,9} This is explained by the fact that the lattice oxide ions surrounding Ba are strong bases effective in producing NO_2^- from NO. Also, the layered structure plays a key role in accommodating a large amount of NO without structural deterioration.

The crystal structure of the double layered cuprate, $\text{La}_2\text{SrCu}_2\text{O}_6$, is composed of oxygen defect intergrowth between double pyramidal copper layers and rock salt type layers (Fig. 1).^{13,16} In the $\text{La}_{2-x}\text{Ba}_x\text{SrCu}_2\text{O}_6$ system, Ba and La are considered to be situated in the interlayer [La/Sr(1) site] between the basal planes of the CuO_5 sheets, where NO intercalation takes place. Part of lanthanum can also be replaced by other divalent cations as has been reported for $\text{La}_{2-x}\text{Ca}_{1+x}\text{Cu}_2\text{O}_6$ ¹⁷ and $\text{La}_{2-x}\text{Sr}_{1+x}\text{Cu}_2\text{O}_6$,¹⁸ but their

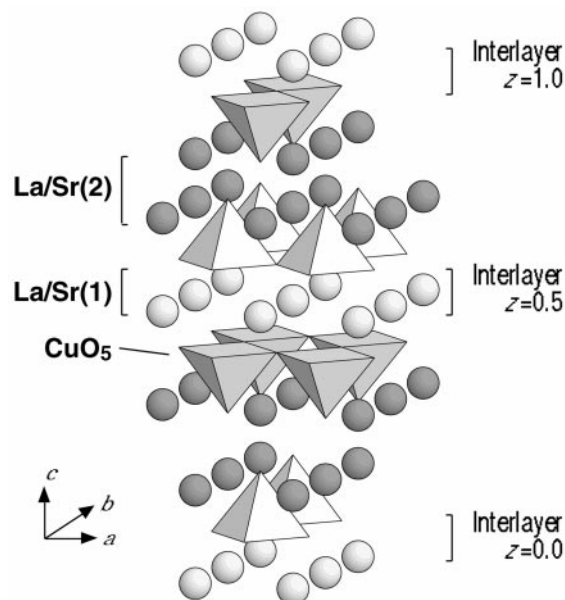


Fig. 1 Crystal structure of double layered cuprate.

effects have not been studied with regard to NO storage properties. In the present study, we have studied the NO reactivity of another possible substituted system with Sr, $\text{La}_{2-x}\text{Sr}_{1+x}\text{Cu}_2\text{O}_6$. Because of the similar ionic radii of La^{3+} and Sr^{2+} , a large extent of solid solution is expected to be obtained. We describe the sorption and desorption properties of NO in comparison with those of the $\text{La}_{2-x}\text{Ba}_x\text{SrCu}_2\text{O}_6$ system to elucidate the role of alkaline earth elements and the layered structure in solid-gas reactions.

Experimental

The double layered cuprate with a composition of $\text{La}_{2-x}\text{Sr}_{1+x}\text{Cu}_2\text{O}_6$ ($0 \leq x \leq 2.0$) was prepared by calcining powder mixtures of oxides and carbonates (La_2O_3 , CuO and SrCO_3 , 99.99%, Rare Metallic Co., Ltd) at 1050 °C in air. A calcined sample was treated with saturated water vapor (*ca.* 20 kPa) at 60 °C for 48 h to accelerate NO absorption. Prior

to the NO reaction, the sample thus prepared was pressed and then crushed into granules of *ca.* 20 mesh.

The crystal structure of the sample was determined by powder X-ray diffraction (XRD, Shimadzu XD-D1) using Cu-K α radiation (30 kV \times 30 mA). The sorption/desorption property of NO was characterized by means of temperature programmed desorption (TPD) in a conventional flow reactor connected to a volumetric vacuum system and to a differential evacuation system. The NO sorption was carried out in the volumetric system by introducing various pressures of NO (99.9%) to the granular sample (0.2 g) held in a quartz tube (8 mm i.d.) at 100–400 °C. Here, the NO uptake by the cuprate sample is expressed in terms of 'mol mol⁻¹', which means 'mol/formula unit of the cuprate'. After NO uptake and subsequent evacuation at room temperature, the sample was heated in a He stream (20 ml min⁻¹) at a constant rate (10 °C min⁻¹). The gas evolution from the sample was analyzed by a quadrupole mass spectrometer (Q-MASS, Monitorr, LEDA-MASS).

Temperature swing sorption/desorption cycles of NO were carried out in a flow system.¹⁵ A water-cooled IR image furnace (ULVAC E-25) was used for alternating the reaction temperature between sorption and desorption steps. The sample bed operated isothermally at 250 °C during each sorption step and at 500, 600 or 700 °C during each desorption step. The termination of each step was followed by a prompt change of the temperature to a next step. During the temperature swing operation, a gaseous mixture of 1 vol% NO–He saturated with water vapor at 20 °C was continuously fed to the granular sample (0.2 g) at a flow rate of 20 ml min⁻¹. The effluent gas was analyzed by gas chromatography (GC, GL Sciences Model370) with a MS-5A column and a chemiluminescence NO_x analyzer (Shimadzu, NOA305).

Results and discussion

Crystal phase analysis

X-Ray diffraction patterns of La_{2-x}Sr_{1+x}Cu₂O₆ (0 \leq x \leq 2.0) after calcination at 1050 °C are compared in Fig. 2. All these patterns are free from reflections due to starting materials, La₂O₃, SrCO₃ or CuO. The diffraction pattern of the unsubstituted

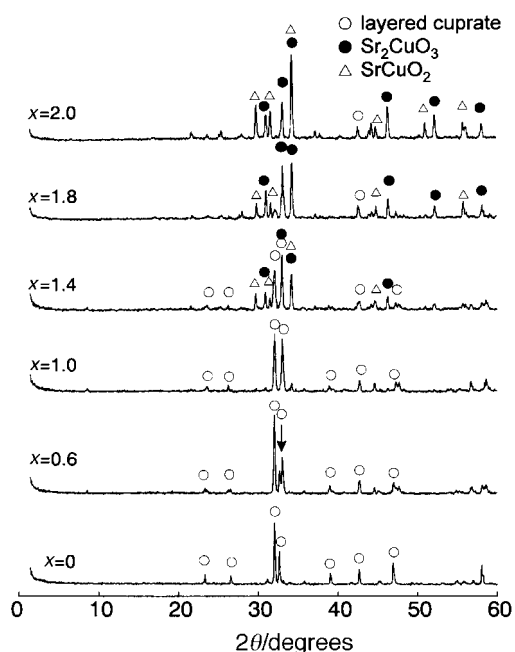


Fig. 2 Powder XRD patterns of La_{2-x}Sr_{1+x}Cu₂O₆ (0 \leq x \leq 2) after calcination at 1050 °C. Precipitation of orthorhombic phase can be seen as splitting of the (110) reflection marked by an arrow.

tuted sample ($x=0$) consisted of a single phase of tetrahedral layered cuprate, La₂SrCu₂O₆ with lattice constants of $a=0.3865$ nm and $c=1.994$ nm. Upon Sr-substitution the original structure was retained up to $x=0.15$, but further substitution led to the splitting of the (110) reflection marked by an arrow in Fig. 2. This can be attributed to the incremental precipitation of orthorhombic layered cuprate, previously reported as La_{1+x}Sr_{2-x}Cu₂O_{5.5+ δ} (0.05 \leq x \leq 0.15) in the phase diagram of the system SrO–La₂O₃–CuO.¹⁹ The crystal structure is derived from that of tetrahedral La₂SrCu₂O₆ with additional ordered oxygen vacancies in the basal copper oxygen plane leading to a superstructure with a tripled b -axis ($b=3a$). The sample in the present study is therefore composed of mixtures of tetrahedral and orthorhombic layered cuprates at 0.2 \leq x \leq 1.0. Further increase of x (x \geq 1.2) caused the precipitation of two binary oxides, Sr₂CuO₃ and SrCuO₂, which became dominant at x \geq 1.8 with simultaneous disappearance of the orthorhombic layered cuprate. At $x=2.0$, a mixture of Sr₂CuO₃ and SrCuO₂ was produced in accord with the reported phase diagram of the SrO–CuO system.²⁰ Since Sr in these pseudo-binary Sr–La oxides cannot be replaced by La,¹⁹ the samples at 1.2 \leq x $<$ 2.0 are mixtures of orthorhombic layered cuprate, Sr₂CuO₃ and SrCuO₂.

NO sorption property

Fig. 3(a) shows the time course of NO uptake by La_{2-x}Sr_{1+x}Cu₂O₆, which was measured in a volumetric vacuum system at 250 °C. As was evident in our previous study, the unsubstituted sample ($x=0$) cannot absorb NO regardless of the reaction temperatures. NO uptake was gradually increased with the Sr-substitution accompanied by incremental precipitation of the orthorhombic layered cuprate phase. The oxygen defective structure and copper vacancies $>2+$ in this phase seems to be effective in promoting NO reactions as in the case of La_{2-x}Ba_xSrCu₂O₆.¹⁴ The cumulative NO uptake and corresponding initial uptake rate [Fig. 3(b)] gave rise to the maximum at $x=1.4$, at which two binary

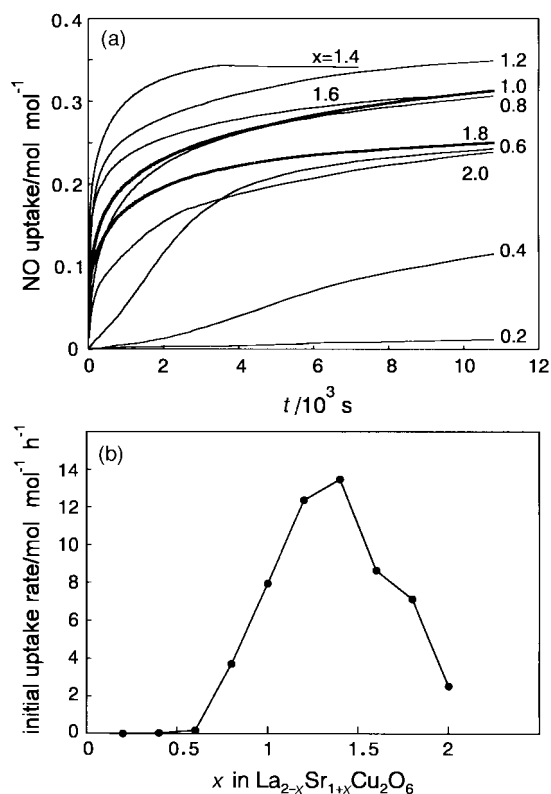


Fig. 3 Time courses (a) and initial rate (b) of NO uptake for La_{2-x}Sr_{1+x}Cu₂O₆ measured in a volumetric vacuum system at 250 °C.

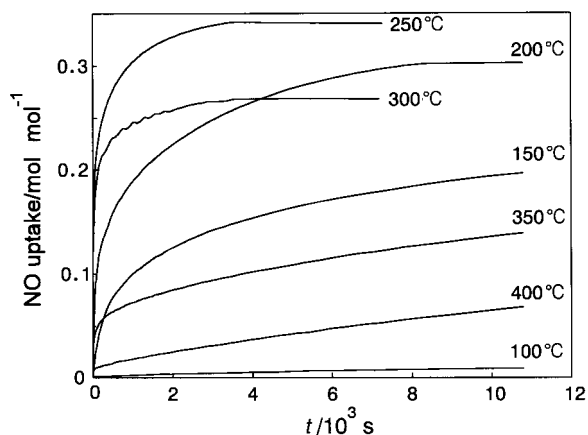


Fig. 4 Time courses of NO uptake for $\text{La}_{0.6}\text{Sr}_{2.4}\text{Cu}_2\text{O}_6$ measured in a volumetric vacuum system at various temperatures.

Sr–Cu oxides were produced in addition to the orthorhombic layered cuprate. According to the phase diagram,¹⁹ it is estimated that the sample with this substitution rate consists of *ca.* 60 mol% orthorhombic layered cuprate, *ca.* 20 mol% Sr_2CuO_3 , and *ca.* 20 mol% SrCuO_2 . Further Sr-substitution ($x \geq 1.5$) resulted in the steep decrease of NO uptake and initial uptake rate in accord with decreasing fraction of the orthorhombic layered cuprate. These results suggest that the NO absorbability is sensitive to not only the composition but also to the crystal structure of the present ternary system. The largest NO uptake of the present system ($0.34 \text{ mol mol}^{-1}$) is less than that of the Ba-substituted system, $\text{La}_{2-x}\text{Ba}_x\text{SrCu}_2\text{O}_6$, for which NO uptake is almost as much as the amount of substituted Ba.¹³

Fig. 4 shows the effect of reaction temperature on the NO uptake ($x=1.4$). NO uptake could be observed above 100°C and increased monotonously up to a maximum at 250°C , at which the highest initial uptake rate was also attained. Above 250°C , however, the NO uptake was steeply decreased as a result of the shift of the equilibrium to desorption.

To determine the mechanism of solid–gas reactions between the sample ($x=1.4$) and NO, the structural change during the NO uptake was studied by XRD measurements (Fig. 5). It is apparent that diffraction peaks of the three cuprate phases were weakened after water vapor treatment at 60°C and subsequent NO uptake ($0.34 \text{ mol mol}^{-1}$) at 250°C . In particular, the most drastic change was observed for reflections of the orthorhombic layered cuprate. As reported previously,¹³ water vapor treatment produces hydroxyl groups bound to metallic species with basic character, *e.g.*, Sr, which play the role as Lewis base for the reaction with gaseous NO_x . In the

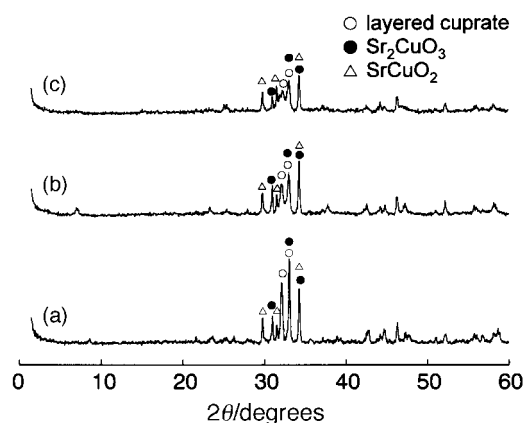


Fig. 5 Change of XRD patterns during NO uptake: (a) dried sample ($x=1.4$), (b) on exposure to water vapor (20 kPa, 60°C , 48 h) and (c) subsequently to NO (13 kPa, 250°C , 160 min).

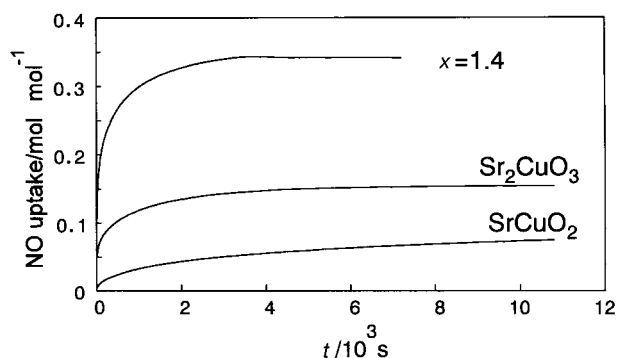


Fig. 6 Time courses of NO uptake for $\text{La}_{0.6}\text{Sr}_{2.4}\text{Cu}_2\text{O}_6$ ($x=1.4$), Sr_2CuO_3 , and SrCuO_2 measured in a volumetric vacuum system at 250°C .

$\text{La}_{2-x}\text{Ba}_x\text{SrCu}_2\text{O}_6$ system, such hydroxyl groups are generated in the interlayer so that a significant expansion of the lattice parameter was observed. Similar structural change was also observed in the present system as a shift of the (002) reflection from $2\theta=8.76$ to 7.01° as shown in Fig. 5(a) and (b). This corresponds to a change of interlayer distance from 1.01 to 1.26 nm caused by water vapor treatment. Unlike the Ba-substituted sample, however, subsequent NO uptake into the present sample ($x=1.4$) did not lead to a further increase of interlayer distance [Fig. 5(c)]. These results imply that the orthorhombic layered cuprate phase is responsible for the NO sorptive property of the $\text{La}_{2-x}\text{Sr}_{1+x}\text{Cu}_2\text{O}_6$ system, but neither intercalation of NO nor the precipitation of nitrate/nitrite phases was evident from XRD measurements. To confirm this conclusion, NO uptake was conducted for monophasic samples of a mixture of two binary oxides, Sr_2CuO_3 and SrCuO_2 , which were prepared by calcining stoichiometric mixtures of SrCO_3 and CuO at 900°C . As shown in Fig. 6, these binary oxides showed much less NO uptake as compared to the sample with $x=1.4$. Thus, the binary oxides are considered to play a secondary role in NO uptake into the orthorhombic layered cuprate, as discussed later.

IR absorption spectra were recorded to analyze the chemical structure of the sample ($x=1.4$) before and after NO uptake (Fig. 7). After exposing the sample to NO at 250°C , absorptions appeared at 1420 , 1280 and 820 cm^{-1} , which are ascribable to N–O stretching modes of NO_2^- and NO_3^- ions.²¹ Their intensities increased with increasing amount of NO uptake, suggesting that NO is absorbed as nitrite and nitrate ions in the solid.

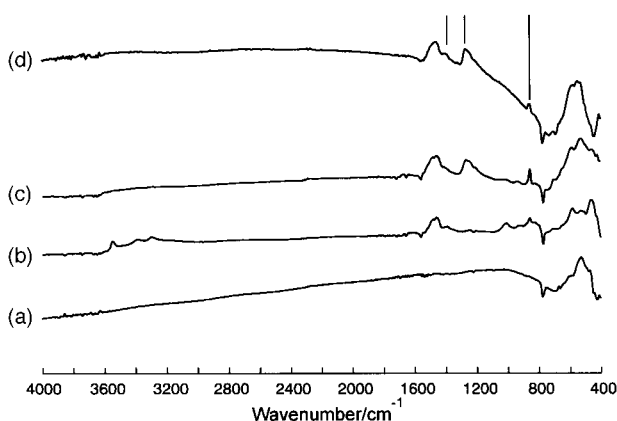


Fig. 7 FTIR spectra after water vapor treatment: (a) as treated sample ($x=1.4$), (b) after evacuation at 250°C , (c) after exposure to NO (6.5 kPa, 250°C , 60 min), (d) after exposure to NO (13 kPa, 250°C , 60 min).

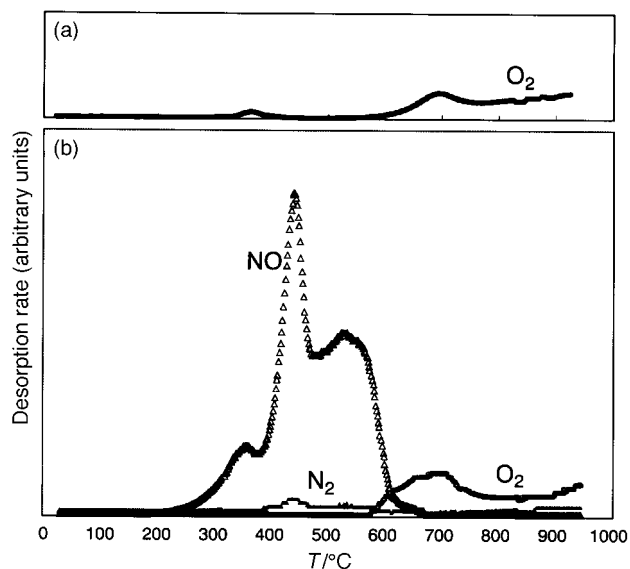


Fig. 8 TPD profiles from the sample ($x=1.0$) after absorbing (a) 0.0 and (b) 0.30 mol mol⁻¹ of NO at 250 °C. Heating rate, 10 °C min⁻¹; carrier gas, He.

Temperature programmed desorption of NO

Fig. 8 shows TPD profiles of the single phase of orthorhombic layered cuprate ($x=1.0$) as prepared and after subsequent NO uptake. The sample treated with water vapor showed only spontaneous O₂ desorption [Fig. 8(a)]. This oxygen evolution is attributable to the desorption of lattice oxygens, accompanied by partial reduction of copper ions (probably Cu³⁺). The desorption profile after NO uptake of 0.30 mol mol⁻¹ at 250 °C mainly consisted of NO (200–600 °C) and O₂ (>580 °C) [Fig. 8(b)]. Considering that the amount of O₂ desorption was not changed by NO uptake and that the formation of N₂ was very small, we can conclude that NO incorporated by the cuprate was liberated reversibly. The corresponding TPD profiles were also obtained from the sample ($x=1.4$), which showed the largest NO uptake. As shown in Fig. 9(a), the as prepared sample showed less O₂ desorption as compared to that from the sample with $x=1.0$. This is simply due to more oxygen-deficient structure of the

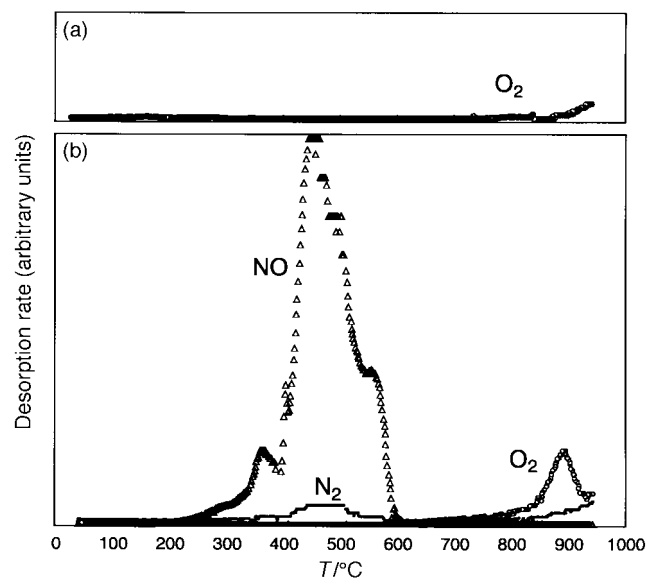


Fig. 9 TPD profiles from the sample ($x=1.4$) after absorbing (a) 0.0 and (b) 0.34 mol mol⁻¹ of NO at 250 °C. Heating rate, 10 °C min⁻¹; carrier gas, He.

orthorhombic layered cuprate caused by further Sr-substitution. In addition, coexisting binary oxides themselves were found not to eliminate the lattice oxygen up to 950 °C under the same conditions. The TPD profile after NO uptake of 0.34 mol mol⁻¹ was basically the same as in Fig. 8(b), but, in this case, O₂ desorption at >750 °C was obviously larger than expected [Fig. 9(a)]. This additional O₂ desorption can not be explained by reversible desorption of NO, suggesting that oxidative NO sorption takes place at $x=1.4$. This is consistent with the results of FTIR measurements, which showed the formation of nitrate species after NO uptake (Fig. 7). The NO desorption properties of the present system are in contrast to that of the La_{2-x}Ba_xSrCu₂O₆ system, which exhibits dissociative desorption of NO as N₂.^{11,14}

As revealed in the preceding section, the maximum NO uptake of the present system was attained for the sample ($x=1.4$) consisting of the orthorhombic layered cuprate and two binary oxides. Although the former is responsible for the rapid NO uptake, the role of the latter has not been defined. However, the TPD results mentioned above give an insight into how these coexisting oxides promote NO uptake into the layered cuprate. As can be judged from comparison between Fig. 8 and 9, NO is oxidatively sorbed in the presence of binary oxides. This means that the binary oxides play a role as oxidizing agents, which convert gaseous NO to NO₂ prior to sorption into the layered cuprate. It is clear that the layered cuprate shows much higher reactivity towards NO₂ than NO. Also, we have already reported a similar effect in the BaCuO₂/CuO system for NO uptake reactions.^{1,9} In that case, the NO adsorbability of BaCuO₂ is much improved by mixing with CuO, which facilitates the oxidation of NO to NO₂ promoting solid-gas reactions to produce barium nitrate.

Temperature swing NO sorption/desorption

The sample ($x=1.4$) was submitted to temperature swing NO sorption/desorption cycles in a conventional flow reactor. In such experiments, heating of the sample at 250 °C for a sorption step and at 500, 600 or 700 °C for a desorption step was repeated in a stream of 1 vol% NO-He (20 ml min⁻¹) saturated with water vapor at 20 °C. The total NO feed during each sorption step corresponds to 0.40 mol mol⁻¹. Three typical results are shown in Fig. 10 as the change of NO concentration in the effluent gas during the temperature swing cycles. In the first cycle, almost complete removal of NO occurred during 20 min of the sorption step, but adsorbability after the second cycle was decreased, the extent of this depending on the desorption temperature. NO oxidation over the binary oxides should consume lattice oxygens in the absence of gaseous O₂. However, it is expected that these oxides become more resistant to reduction with further sorption/desorption cycles. This is a possible reason why the highest adsorbability was attained in the first step. At the end of each sorption step, the temperature was raised to the desorption temperatures and NO stored in the solid was immediately condensed out of the stream. The sorption/desorption characteristics were strongly dependent on the desorption temperature, the effect of which could be observed on the concentration of desorbed NO and the regeneration capacity for NO. An increase in the desorption temperature increased the desorption rate and thus the maximum concentration of NO in the effluent. A maximum concentration of NO_x (NO + NO₂) in the effluent was 10 times higher than that of NO in the influent on desorption steps at 700 °C. By contrast, higher desorption temperatures led to lower regeneration capacities as evident from decreased NO removal after the second cycle. Since the regenerative capacity for NO also became smaller when the reaction was conducted in the absence of water vapor, the deterioration of NO removal is caused by thermal elimination of hydroxyl groups from the solid surface.

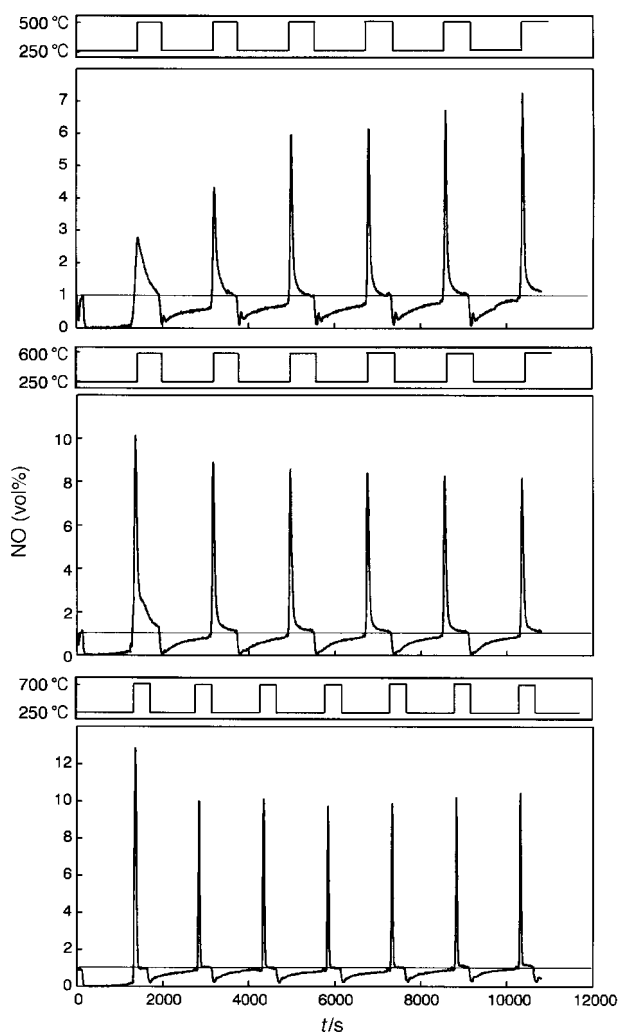


Fig. 10 Temperature swing sorption/desorption cycles of NO ($x=1.4$). Temperatures for sorption/desorption; 250/500 °C, 250/600 °C, 250/700 °C, 1 vol% NO-He, 20 ml min⁻¹, sample, 0.2 g.

Comparison of NO reactivity of Ba- and Sr-substituted layered cuprates

The present study has revealed that Sr-substituted layered cuprate, $\text{La}_{2-x}\text{Sr}_{1+x}\text{Cu}_2\text{O}_6$, shows NO sorbability similarly to $\text{La}_{2-x}\text{Ba}_x\text{SrCu}_2\text{O}_6$ in our previous studies.^{11–15} Table 1 compares the NO reactivity of these two different substituted cuprates, $\text{La}_{2-x}\text{A}_x\text{SrCu}_2\text{O}_{6-\delta}$ (A = Sr and Ba). The NO uptake of both systems is brought about by replacing the La site by alkaline earth elements, Ba or Sr. From a chemical view point, their strong basicity is effective in bringing about interactions with NO molecules. However, the maximum NO uptake for M = Sr (0.34 mol mol⁻¹) was far lower than that for M = Ba. This can be explained by the lower basicity of Sr as compared to Ba. On the other hand, the substitution of La for alkaline earth elements leads to structural modification as a result of

Table 1 NO reactivity of $\text{La}_{2-x}\text{A}_x\text{SrCu}_2\text{O}_{6-\delta}$ (A = Sr or Ba)

A	Maximum uptake ^a /mol mol ⁻¹	Reaction product	Desorption species
Sr	0.34 ($x=1.4$)	Precipitation as NO_3^- and NO_2^-	NO_x (200–600 °C) O_2 (> 750 °C)
Ba	$\approx x^b$	Intercalation as NO_2^- ($x \approx 0.5$)	NO_x (250–670 °C) O_2 (> 580 °C), N_2 (> 800 °C)

^aAt 250 °C. ^bThe uptake is almost equal to x , the amount of Ba.

charge compensation. The substitution of La^{3+} for these divalent cations produces Cu^{3+} ,^{11,19} which will facilitate oxidative NO uptake into the solid phase. It also should be noted that the charge compensation process results in an oxygen-defective superstructure as was observed in previously characterized samples with high NO sorbability, e.g., $\text{LaSr}_2\text{Cu}_2\text{O}_{6-\delta}$ ($a \times 3a$)¹⁹ and $\text{La}_{1.5}\text{Ba}_{0.5}\text{SrCu}_2\text{O}_{6-\delta}$ ($3a \times 3a$).¹³

A significant point is that NO sorption into the M = Sr sample is unlikely to be caused by intercalation which dominates for M = Ba and is characterized by the dissociative desorption of NO as N_2 . As shown in Fig. 5, the NO uptake for M = Sr resulted in considerable structural destruction probably due to the precipitation of amorphous strontium nitrite and nitrate. These precipitates should be decomposed to eliminate only NO_x and O_2 at elevated temperatures and is a reason why dissociative desorption of NO did not occur from the M = Sr samples. Although the factor controlling these NO sorption mechanisms is not clear at this stage, it is possibly related to the ionic radii of the substituted ions, Sr and Ba. In the ideal double layered structure (Fig. 1), Ba^{2+} as well as Sr^{2+} occupy the La/Sr(1) site in the interlayer.¹³ Owing to its larger ionic radius, Ba^{2+} should lead to larger interlayer spacing between the CuO_5 sheets so that NO molecules can be accommodated more readily. Our preliminary results have demonstrated that intercalation cannot proceed in a Ca-substituted system, $\text{La}_{2-x}\text{Ca}_x\text{SrCu}_2\text{O}_6$. In view of the basicity and ionic radii of A, the NO reactivity of $\text{La}_{2-x}\text{A}_x\text{SrCu}_2\text{O}_6$ is expected to decrease in the sequence of A = Ba > Sr > Ca.

Conclusions

The following conclusions have emerged from this study.

(1) The NO uptake into $\text{La}_{2-x}\text{Sr}_{1+x}\text{Cu}_2\text{O}_6$ was maximum at $x=1.4$, at which a mixture of three different phases of orthorhombic layered cuprate, Sr_2CuO_3 and SrCuO_2 was produced. The latter two phases appear to be effective in oxidation of NO to NO_2 and thus promote solid-gas reactions with a layered cuprate to produce nitrate and nitrite precipitates.

(2) Heating the sample ($x=1.4$) after NO uptake led to NO desorption at 200–600 °C and desorption of O_2 at > 750 °C, but dissociative desorption of N_2 was not observed. The sample demonstrated temperature swing NO sorption/desorption cycles in a stream of 1 vol% NO-He.

(3) The different NO reactivities of $\text{La}_{2-x}\text{A}_x\text{SrCu}_2\text{O}_6$ (A = alkaline earth metal) are associated with the ionic radius and basicity of substituents A.

Acknowledgements

The present study was supported in part by a Grant-in Aid for Scientific Research from the Ministry of Education, Science, Sports, and Culture (09750926 and 10555282).

References

- H. Arai and M. Machida, *Catal. Today*, 1994, **22**, 97.
- G. E. Keller, *Chem. Eng. Prog.*, 1995, **91**, 56.
- N. Miyoshi, S. Matsumoto, K. Katoh, T. Tanaka, J. Harada, N. Takahashi, K. Yokota, M. Sugiura and K. Kasahara, *SEA Paper*, 1995, 950809.
- E. Fridell, M. Skoglundh, S. Johansson, B. Westberg, A. Törncrena and G. Smedler, *Catalysis and Automotive Pollution Control IV*, ed. N. Kruse, A. Frennet and J.-M. Bastin, Elsevier, Amsterdam, 1998, p. 537.
- H. Shimada, S. Miyama and H. Kuroda, *Chem. Lett.*, 1988, 1797.
- K. Tabata, H. Fukui, S. Kohiki, N. Mizuno and M. Misono, *Chem. Lett.*, 1988, 799.
- N. Mizuno, Y. Fujisawa and M. Misono, *J. Chem. Soc., Chem. Commun.*, 1989, 316.
- M. Machida, K. Yasuoka, K. Eguchi and H. Arai, *J. Chem. Soc., Chem. Commun.*, 1990, 1165.

- 9 M. Machida, S. Ogata, K. Yasuoka, K. Eguchi and H. Arai, *Proc. 10th Int. Cong. Catal.*, 1992, 1645.
- 10 S. Hodjati, P. Bernhardt, C. Petit, V. Pitchon and A. Kiennemann, *Appl. Catal. B: Environ.*, 1998, **19**, 209, 221.
- 11 M. Machida, H. Murakami, T. Kitsubayashi and T. Kijima, *J. Mater. Chem.*, 1994, **4**, 1621.
- 12 M. Machida, H. Murakami and T. Kijima, *J. Chem. Soc., Chem. Commun.*, 1995, 485.
- 13 M. Machida, H. Murakami, T. Kitsubayashi and T. Kijima, *Chem. Mater.*, 1996, **8**, 197.
- 14 M. Machida, H. Murakami, T. Kitsubayashi and T. Kijima, *Chem. Mater.*, 1997, **9**, 135.
- 15 M. Machida, H. Murakami, T. Kitsubayashi and T. Kijima, *Appl. Catal. B: Environ.*, 1996, **17**, 195.
- 16 N. Nguyen, L. Er-Rakho, C. Michel, J. Choisnet and B. Raveau, *Mater. Res. Bull.*, 1980, **15**, 891.
- 17 K. Kinoshita, H. Shibata and T. Yamada, *Physica C*, 1990, **171**, 523.
- 18 V. Caignaert, N. Nguyen and B. Raveau, *Mater. Res. Bull.*, 1990, **25**, 199.
- 19 D. M. De Leeuw, C. A. H. A. Mutsaers, G. P. J. Geelen and C. Langereis, *J. Solid State Chem.*, 1989, **80**, 276.
- 20 H. Müller-Buschbaum, *Angew. Chem.*, 1977, **89**, 704.
- 21 K. Nakamoto, *Infrared and Raman Spectra of Inorganic and Coordination Compounds*, Wiley, New York, 4th edn., 1986, p. 476.

Paper 8/09939A